JOURNAL OF MATERIALS SCIENCE 30 (1995) 4591–4597

Mg–Zn–Al–CO_3 and Zn–Cu–Al–CO_3 hydrotalcite-like compounds: preparation and characterization

F. KOOLI*, K. KOSUGE, A. TSUNASHIMA
Materials Processing Department, National Institute for Resources and Environment, 16–3 Onogawa, Tsukuba 305, Japan

A series of *M*–Zn–Al (*M*=Mg, Cu) double hydroxide phases with carbonate anion were prepared by coprecipitation of 333 K, from the corresponding nitrate solution and sodium carbonate aqueous solution at pH 10. The characterization and properties of the products were investigated. It seems that reactivity of aluminium ions into the host layer depends on the identity of coexistent divalent cations (magnesium or copper), and the thermal properties of this layer at relatively high temperatures also depend on the nature of divalent cations.

1. Introduction

Hydrotalcite and related minerals, as well as synthetic hydrotalcite-like compounds, have the general chemical formulae $M_{1-x}M'_x(OH)_2A_{x/n}mH_2O$, where M is a divalent cation, such as Mg, Zn, Ni, ..., and M' is a trivalent cation, such as Al, Cr, Fe, ..., A^{n-} is an anion like Cl^-, NO_3^-, SO_4^{2-}, CO_3^{2-}, ..., and x mainly lies in the range 0.16–0.33 [1–3]. Thevenot *et al.* [4] obtained zinc–aluminium hydrotalcite-like compounds with x in the range 0.33–0.44. The general formulae should be extended to include a monovalent cation in the octahedral position [5]. The structure of hydrotalcite-like compounds consists of a brucite layer charged positively resulting from the substitution of a trivalent cation by a divalent cation, and a negatively charged interlayer containing exchangeable anions and water molecules [6]. These layers can be stacked with two different symmetries: hexagonal symmetry, with two layers per unit cell, and rhombohedral symmetry with three layers per unit cell [2, 7]. An abounding literature exists on the compositions and structures of these materials, in general with one mono- or divalent cation and one trivalent cation. Only a few systems composed of the admixture of two divalent cations and aluminium appear in nature [8]. Such systems were investigated for the preparation of industrial catalysts [9], because thermal transformation and decomposition lead to catalytically active metal oxides.

In the present study, various Mg–Zn–Al and Zn–Cu–Al hydroxide carbonate compounds were synthesized, and the influence of Zn/Mg or Cu/Zn and $(M + Zn)$ /Al ratios (with M = Mg or Cu) on the nature of the obtained coprecipitates were investigated. X-ray diffraction, infrared analysis and thermal properties are also reported.

2. Experimental procedure

2.1. Sample preparation

The two double hydroxide carbonate layered systems were prepared as described previously [10]. The *M*–Zn–Al solid solution was formed by coprecipitation at 333 K from magnesium or copper, zinc and aluminium nitrate solutions, added dropwise into 100 cm^3 of 1 *M* sodium carbonate solution with constant stirring. The pH was kept constant at ten by separate addition of a 3 N NaOH solution. The coprecipitates were aged in their mother liquor at 333 K for 1 h, filtered and washed with 1 l of boiled distilled water, then dried at 320 K for 24 h.

2.2. Measurements

The amounts of Mg^{2+}, Zn^{2+}, Cu^{2+} and Al^{3+} in the products were measured by X-ray fluorescence (XRF) with a Rigaku 3030 X-ray spectrometer. For the characterization of the obtained phases and the determination of the unit cell parameters, a Rigaku RU300 equipped with CuK_α radiation and a nickel filter was employed. Combined thermogravimetric (TGA) and differential thermal analysis (DTA) were carried out with a Rigaku apparatus at a heating rate of 15 °C min^{-1} in air using 5–6 mg of sample. Fourier Transform infrared (FTIR) analysis was performed with a Jeol JIR 3510 FTIR spectrophotometer, using a small amount of sample mixed with KBr, and was recorded in the 4000–400 cm^{-1} region.

To study the properties of the thermally treated materials, 0.5 g of sample were calcined in air, for 2 h at various temperatures in the range 473–1273 K with a Thermolyne 10 500 furnace.

* Present address: Department of Chemistry, University of Cambridge, Lensfield Road, Cambridge CB2 1EW, UK. Author to whom all correspondence should be addressed.

0022–2461

TABLE I Chemical analysis results of the samples and lattice parameters of the hydrotalcite structure phase in the Mg–Zn–Al system: (S) sample name, (Theo) theoretical, (Exp) experimental, (HT) hydrotalcite, (Daw) dawsonite, (ZnO) zinc oxide.

	Zn/Mg [a]		(Mg + Zn)/Al [a]			Unit cell parameters (nm)	
S	Theo.	Exp.	Theo.	Exp.	Phase[b]	*a*	*c*
M1	0.00	0.00	1.00	1.45	HT, Daw	0.3032	2.3034
M2	0.00	0.00	2.00	2.10	HT	0.3048	2.2926
M3	0.00	0.00	3.00	2.94	HT	0.3062	2.2382
Z1	0.10	0.10	1.00	1.19	HT, Daw	0.3034	2.2926
Z2	0.10	0.10	2.00	2.39	HT, Daw	0.3050	2.3025
Z3	0.10	0.10	3.00	3.06	HT	0.3068	2.3430
Z4	0.10	0.09	4.43	4.95	HT	0.3074	2.3783
Z5	0.10	0.11	5.98	5.88	HT	0.3082	2.4219
Z6	1.00	0.88	1.00	1.33	HT	0.3040	2.2671
Z7	1.00	0.86	2.24	2.09	HT	0.3058	2.2845
Z8	1.00	0.87	4.00	3.82	HT, ZnO	0.3071	2.3511
Z9	1.00	0.85	6.02	5.39	HT, ZnO	0.3082	2.3679
Z10	0.20	0.22	3.00	3.07	HT	0.3072	2.3511
Z11	0.50	0.52	3.00	3.14	HT	0.3070	2.3451
Z12	0.80	0.74	3.00	2.83	HT	0.3070	2.3205
Z13	2.00	1.70	3.00	2.80	HT	0.3076	2.3064
Z14	4.00	3.05	3.00	2.49	HT, ZnO	0.3070	2.2905
Z15	6.00	4.34	3.00	2.35	HT, ZnO	0.3072	2.2877
Z16	10.00	8.10	3.00	3.06	HT, ZnO	0.3070	2.2877

[a] Atomic ratio.
[b] As-detected by PXRD.

3. Results and discussion

3.1. Chemical analysis

All the Mg–Zn–Al and Zn–Cu–Al powders were white and slightly blue, respectively.

The results on the Mg–Zn–Al system having various Zn/Mg and (Mg + Zn) /Al ratios are presented in Table I. In the case of Mg–Al solid solutions (samples M1–M3), the experimental values of the Mg/Al ratios are approximately equal to the theoretical values, i.e. in solution, except for Mg/Al equal to one, where the experimental value is higher than the theoretical one, which means that aluminium does not precipitate as well as magnesium.

In the Mg–Zn–Al system, with a theoretical Zn/Mg ratio around 0.10, the experimental values of Zn/Mg are always equal to the theoretical one. The experimental ratios (Mg + Zn) /Al are higher than the theoretical ratio (samples Z1–Z4), except for (Mg + Zn)/Al = 6 where the values is approximately equal (sample Z5). This indicates that aluminium content in the coprecipitate is lower than expected. Brindley and Kikkawa [11] have interpreted the higher experimental values compared to the theoretical ratios, in the case of the Mg–Al system, by a smaller preference of aluminium cations in the crystalline products than in the coexisting solutions. Similar results were obtained in the Mg–Zn–Al–sulphate solid solution [10].

When the Zn/Mg ratio increases, the experimental values of Zn/Mg and (Mg + Zn) /Al are always smaller than the theoretical ratios, except for (Mg + Zn)/Al = 1. The XRF analysis showed a large variation in the zinc content between the solid solutions, as compared to that of the liquid solutions, which is not the case for magnesium. This fact can be explained by the lower reactivity of zinc ion during the coprecipitation.

The chemical analysis results of the Zn–Cu–Al system are presented in Table II. In the Zn–Al system (samples A1–A3), the experimental values of the Zn/Al ratios are always smaller than the theoretical values, which can be due to the lower reactivity of zinc ion during the coprecipitation. This is in agreement with the results observed in the previous system *vide supra.*

Whatever is the quantity of copper added, the experimental ratio (Zn + Cu)/Al is this time always higher than the theoretical ratio, this behaviour is due to the lower reactivity of aluminium during coprecipitation. These results are in good agreement with the studies of Doesburg *et al.* [12]. The experimental Cu/Zn ratios are smaller than the theoretical values for the high copper content (samples C13–C16). In this case the reactivity of the copper ion is smaller than the reactivity of the zinc cation.

The behaviour of zinc ion depends on the identity of the other divalent cation. At high zinc content, it precipitates easily in the Zn–Cu–Al system, however, in the Mg–Zn–Al system, precipitation is not complete. But previous studies emphasized that synthesized compounds have generally cationic proportions very similar to those of the starting solutions in the case of one di- and trivalent cation [13].

3.2. Powder X-ray diffraction (XRD)

The PXRD analysis showed that most of the samples were composed of pure hydrotalcite compounds; however, in some cases zinc oxide and dawsonite [$NaAlCO_3(OH)_2$] phases were also detected. The PXRD patterns of carbonate phases for the two systems were similar to those of hydrotalcite-like compounds with sharp and symmetrical peaks, and some asymmetrical peaks (Fig. 1). The values of unit cell

TABLE II Chemical analysis results of the samples and lattice parameters of the hydrotalcite structure phase in the Zn–Cu–Al system: (S) sample name, (Theo) theoretical, (Exp) experimental, (HT) hydrotalcite, (Daw) dawsonite, (ZnO) zinc oxide.

	Cu/Zn [a]		(Zn + Cu)/Al [a]			Unit cell parameters (nm)	
S	Theo.	Exp.	Theo.	Exp.	Phase[b]	*a*	*c*
A1	0.00	0.00	1.15	1.01	HT	0.3056	2.2656
A2	0.00	0.00	2.00	1.48	HT	0.3066	2.2692
A3	0.00	0.00	3.00	2.41	HT, ZnO	0.3070	2.2722
C1	0.11	0.11	0.80	1.04	HT	0.3068	2.2608
C2	0.11	0.13	1.61	1.83	HT	0.3076	2.2718
C3	0.11	0.12	2.42	2.78	HT, Daw	0.3078	2.2767
C4	0.11	0.12	3.21	3.80	HT, Daw	0.3086	2.2794
C5	0.11	0.12	4.80	5.98	HT, Daw	0.3090	2.2794
C6	1.11	1.00	0.84	1.11	HT, Daw	0.3074	2.2560
C7	1.12	1.11	1.68	1.87	HT	0.3078	2.2620
C8	1.12	1.16	3.39	3.90	HT, ZnO	0.3086	2.2746
C9	1.12	1.15	5.03	5.63	HT, ZnO	0.3102	2.2650
C10	0.22	0.22	2.68	2.71	HT	0.3078	2.2716
C11	0.56	0.59	2.49	3.06	HT	0.3088	2.2698
C12	0.89	0.94	2.51	3.02	HT	0.3090	2.2980
C13	2.23	2.03	2.54	2.82	HT	0.3090	2.2716
C14	4.45	3.93	2.62	2.96	HT	0.3090	2.2682
C15	6.70	5.88	2.63	2.84	HT	0.3089	2.2608
C16	11.27	9.50	2.64	2.77	HT	0.3100	2.2597

[a] Atomic ratio.
[b] As-detected by PXRD.

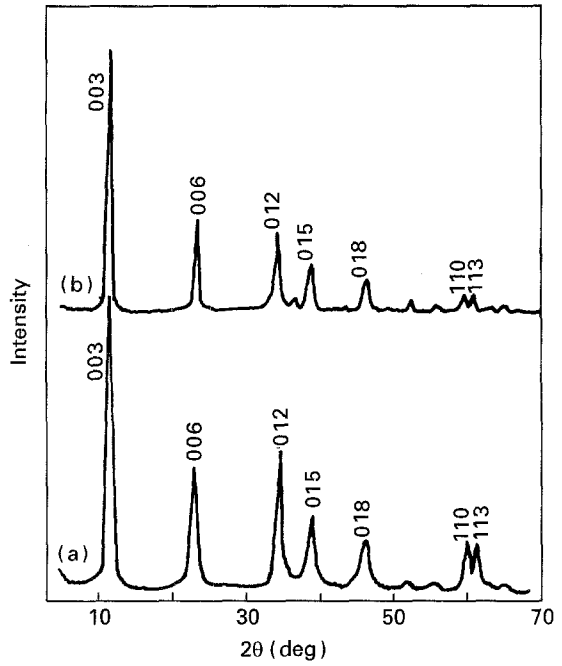

Figure 1 Powder X-ray diffraction patterns of (a) sample Z10, and (b) sample C10.

parameters, which are interpreted in the rhombohedral symmetry, where the *c* parameter corresponds to three times the thickness of one brucite layer [14].

For the Mg–Zn–Al system, the PXRD results are presented in Table I. In the case of the Mg–Al system (samples M1–M3), the value of the *a* parameter decreases with increasing aluminium content in the solid solution. This fact can be explained by the substitution of larger Mg^{2+} ions by smaller Al^{3+} ions [15]. The value of the *c* parameter also decreases with increasing aluminium content. These results are in agreement with the results of Brown and Gastuche [16] and Mascolo and Marino [17].

With small quantities of zinc, the powders formed are pure hydrotalcite-like compounds, except when (Mg + Zn)/Al = 1 (sample Z1), where a small amount of dawsonite [$NaAlCO_3(OH)_2$] phase was detected. The *a* and *c* parameters decrease when the aluminium content increases in the synthesized hydrotalcite powders. The *a* values in the presence of zinc are higher than the *a* values in the Mg–Al system. The decrease of *a* is due to the larger radius of zinc (0.074 nm) and magnesium (0.065 nm) compared to aluminium (0.50 nm) [18].

For higher quantities of zinc (Zn/Mg = 1), the value of the *a* parameter still decreases. For (Mg + Zn)/Al higher than three, a zinc oxide phase was formed with the hydrotalcite phase (samples Z8, Z9). The *c* parameter also decreases when the zinc content increases, but this mainly depends on the nature and steric requirements of the anions and the content of water molecules in the interlayer [14, 19].

In the case of (Mg + Zn)/Al = 3 and when the Mg/Zn ratio varied from 0.2 to 10, a zinc oxide phase was also formed with hydrotalcite when Zn/Mg was higher than four (samples Z14–Z16). It seems that substitution of magnesium by zinc does not affect the value of *a*. This value remains constant around 0.3070 nm, which means that not all the zinc cations were precipitated, and confirms the results of XRF described above. Nevertheless, the value of the *c* parameter decreases. The decrease of the *c* parameter also can be affected by the nature and steric requirements of the carbonate anions in the interlamellar space. This can probably be due to the drying conditions, so leading to a variation of the intercalated water content.

The PXRD results of the Zn–Cu–Al system are presented in Table II. In the case of the Zn–Al system (samples A1–A3), decrease of the parameters *a* and *c* is

also related to the increase of the aluminium content in the solid solution. This behaviour is due to the smaller size of aluminium compared to the zinc ion, and to an increase of electrostatic interaction between the brucite-like layer and the carbonate anions [11].

For a small quantity of added copper, the parameters a and c continue to decrease with increasing aluminium content in the powders. The formation of a dawsonite phase occurred when (Cu + Zn)/Al was higher than two (samples C4, C5). With a Cu/Zn ratio around one, other phases, such as dawsonite at (Cu + Zn)/Al = 1 (sample C6), and ZnO at (Cu + Zn)/Al > 4 were formed with the hydrotalcite-like compounds (samples C8, C9). The values of a and c still decreasing slightly, with the increase of aluminium content in the coprecipitate.

The substitution of zinc by copper increases the value of the a from 0.3070 to 0.310 nm, when (Cu + Zn)/Al is around 2.60 and when the Cu/Zn ratio varies from 0.2 to 11 (samples C10–C16). For all the samples, a pure hydrotalcite-like phase was obtained. Busetto *et al.* [14] and Doesburg *et al.* [12] found a pure hydrotalcite-like phase only when Cu/Zn = 0.5 or one, and when $2.2 < (Cu + Zn)/Al < 3.2$, but their powders were obtained by coprecipitation at pH = 7. The difference of experimental conditions, such as pH, and concentrations of the ion solution, might lead to the observed difference.

3.3. TG and DTA analysis

For the Mg–Zn–Al system the diagrams were quite similar to those of natural hydrotalcite [20], two steps of weight loss were observed (Fig. 2a). The first step is attributed to the loss of physically adsorbed and interlayer water, and the second one to dehydroxylation and loss of CO_2 from the brucite layers. However, with the presence of zinc oxide in the powders at (Mg + Zn)/Al = 3 and Zn/Mg > 4, the TGA diagram showed only one step of weight loss (Fig. 2c) caused by the release of interlayer water, structural water and CO_2 simultaneously around 473–523 K. Similar observation was made in the case of the cobalt-aluminium system [21].

Each weight loss was accompanied by an endothermal transformation (Fig. 2a'). The peak between 343 and 473 K on the DTA curves is attributed to the loss of interlayer water, but the temperature range is smaller than in the Mg–Al system. The decomposition of the host layer and the departure of CO_2 corresponds to the endothermal peak in the range 643–773 K. For some DTA curves (Fig. 2b'), a broad endothermal peak around 523–573 K is recorded. Beck [22] suggested that this peak is due to the loss of structural water bound with the Al ion in the main layer, and Miyata [3] found that this peak is caused by partial dehydroxylation, and its intensity increases with aluminium content in the solid solution.

The TGA and DTA curves for the Zn–Cu–Al system are presented in Fig. 2. The TGA diagrams show the presence of two simultaneous steps of weight loss and another step occurs at relatively high temperature

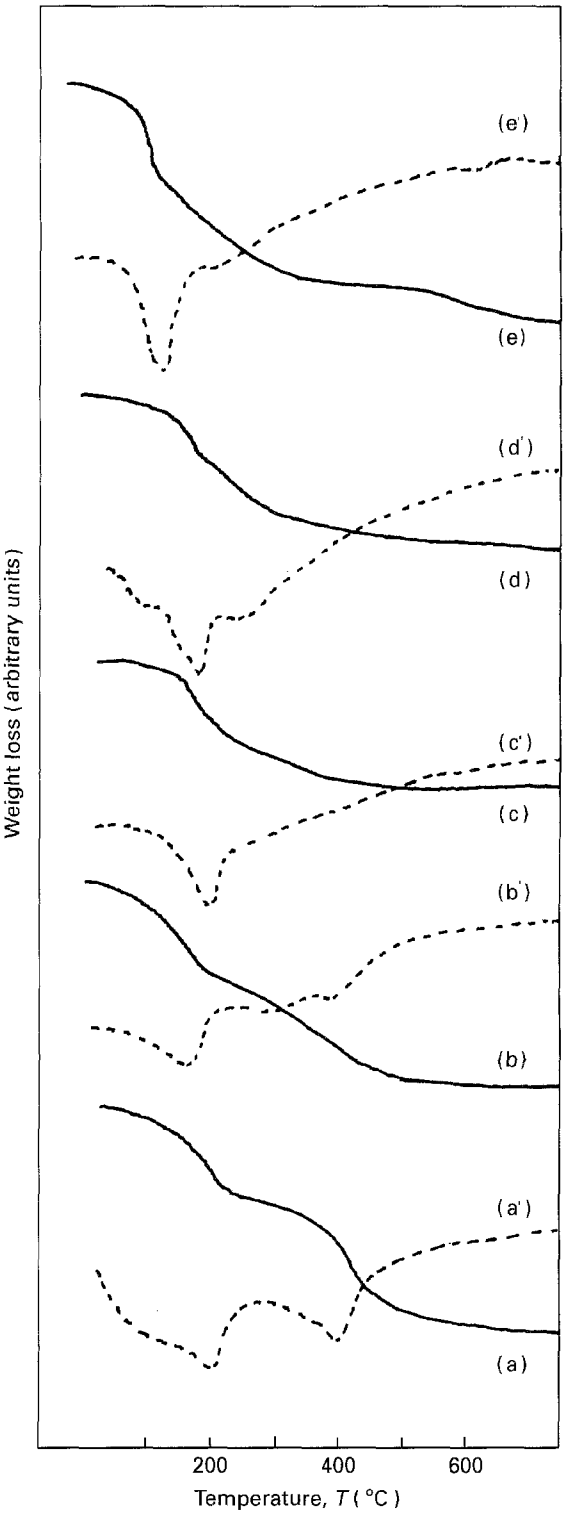

Figure 2 TGA–DTA diagrams of (a, a') sample M3, (b, b') sample Z12, (c, c') sample Z14, (d, d') sample A3, and (e, e') sample C13.

(Fig. 2e). This third step was not observed in the Mg–Zn–Al system. The first step was attributed to the loss of the interlamellar water, and it corresponds also to the first endothermic peak around 423–463 K. The second step was caused by the loss of hydroxyl groups and CO_2 from the brucite layer, and was accompanied by the second endothermic peak in the range 493–513 K. In the range 823–873 K, one cannot explain the presence of the third weight loss, which corresponds to an endothermic peak at 843 K (Fig. 2e'). The exothermic peak at 953 K can be due to the interaction of aluminium cation with the existent metal

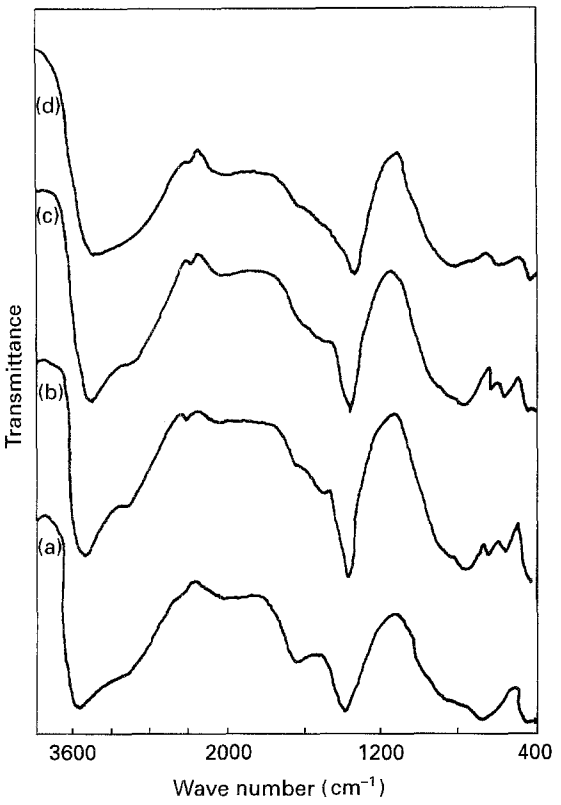

Figure 3 FTIR spectra of (a) sample M3, (b) sample Z12, (c) sample A3, and (d) sample C15.

oxide to form a spinel phase, as observed by PXRD, *vide infra.*

When the zinc content increases in the Mg–Al system, and also the copper content increases in the Zn–Al system, the temperature of the second endothermal peak decreases, this result suggests that the bonding strength between the carbonate anion and the basic brucite-like layer is weakened. Similar results were obtained in the Mg–Zn–Al system with the sulphate anion [10].

3.4. FTIR results

The spectra of the Mg–Al system (Fig. 3a) showed the presence of a strong absorption band in the range 3530–3440 cm^{-1} attributed to the OH stretching mode [$\delta(OH^-)$]; its position shifted to the higher frequency region, with the increase of magnesium and the decrease of aluminium in solid solution, in agreement with the studies of Hernandez–Moreno *et al.* [23]. The shoulder band around 3100–3000 cm^{-1} is due to the hydrogen bond between H_2O molecules and the CO_3 anions in the interlamellar layer [24, 25]. The band around 1640 cm^{-1} is assigned to the free water molecules.

The ν_3 mode of the CO_3^{2-} anion appeared around 1370 cm^{-1}, and shifted also to higher frequency with decreasing aluminium content in the brucite layer. The decrease in the symmetry of the carbonate anion results in a splitting of this band in the case of Mg/Al = 1. Similar results have been reported previously by Bish and Brindley [24] and Hernandez–Moreno *et al.* [23]. The bands around 871 and 670 cm^{-1} are assigned to the ν_2 and ν_4 modes of carbonate anion, respectively; other bands which appear around 760 and 557 cm^{-1} with the increase of aluminium content in solid solution may be assigned to the AlO_6 vibrations [26].

With a small quantity of zinc, the $\delta(OH^-)$ and the ν_3 band of CO_3^{2-} shifts to higher frequency when the aluminium content decreases in the solid solution. When the substitution of magnesium by zinc increases, it affects the position of the ν_3 band, which varies from 1363 to 1384 cm^{-1}; simultaneously the stretching band of OH shifts to higher values. When zinc oxide was formed [(Mg + Zn)/Al > 3 and/or Zn/Mg > 4], the band characteristics of AlO_6 vibrations were clearly observed (Fig. 3b).

For the Zn–Cu–Al system, the spectra are presented in Fig. 3c. In the case of the Zn–Al system, the spectra show a strong absorption band in the 3400–3500 cm^{-1} region, assigned to OH stretching. As in the Mg–Zn–Al system a band around 3100–3000 cm^{-1} is observed. In the region 1400–1300 cm^{-1}, the ν_3 mode of CO_3^{2-} at 1365 cm^{-1} is recorded at Zn/Al = 2 and 3, a split of this band was observed at 1396 and 1359 cm^{-1} with a ratio Zn/Al equal to one. The other bands corresponding to the ν_2 and ν_4 modes of CO_3, and to AlO_6 vibrations, can be attributed clearly. Like the Mg–Al system, the position of the ν_3 mode band shifts slightly to higher frequency when the aluminium content decreases.

When small quantities of copper are present, the position of the ν_3 mode (CO_3^{2-}) shifts to higher frequencies with decreasing aluminium content in the hydrotalcite-like compounds, but are higher compared to the Zn–Al system. When the copper content increases, the position of the main OH band remains around 3450 cm^{-1} and shifts to around 3400 cm^{-1} for Cu/Zn ratios higher than six. The position of the ν_3 mode of CO_3 seems to be unaffected by increasing copper content, varying between 1369 and 1365 cm^{-1} (Fig. 3d), but is affected only by the content of aluminium in the solid solution.

3.5. Thermal properties

In the case of the Mg–Zn–Al system, for all the samples, the departure of interlayer water at 473 K induces a decrease of the interlamellar spacing. At 573 K, the PXRD pattern of hydrotalcite is still present in the Mg–Al system; but in the presence of zinc, the hydrotalcite pattern disappears. Metal oxide phases similar to MgO at Zn/Mg ratio smaller than two, and similar to ZnO at higher Zn/Mg ratios, are simultaneously detected. At 773 K, MgO and ZnO are formed at lower ratios Zn/Mg. When Zn/Mg is higher than two only ZnO is produced. The lattice parameters of the formed metal oxides are slightly smaller than the pure oxides, which indicates substitution of aluminium into the magnesium and/or zinc oxide. The same phases were also obtained at 973 K. (Fig. 4).

At high temperature, between 1023 and 1273 K, the solid solutions of magnesium–aluminium oxide and/or zinc–aluminium oxide decompose to MgO and/or ZnO and a spinel form (MAl_2O_4, M = Mg, Zn). The amount of the latter phase increases with temperature,

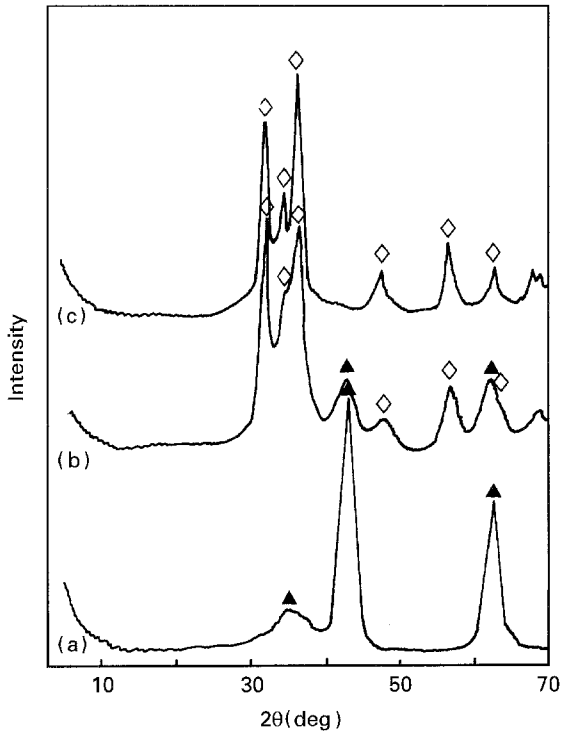

Figure 4 Powder X-ray diffraction patterns of (a) sample M3, (b) sample Z12, and (c) sample Z14 obtained upon calcination at 973 K: (▲) MgO, (◇) ZnO.

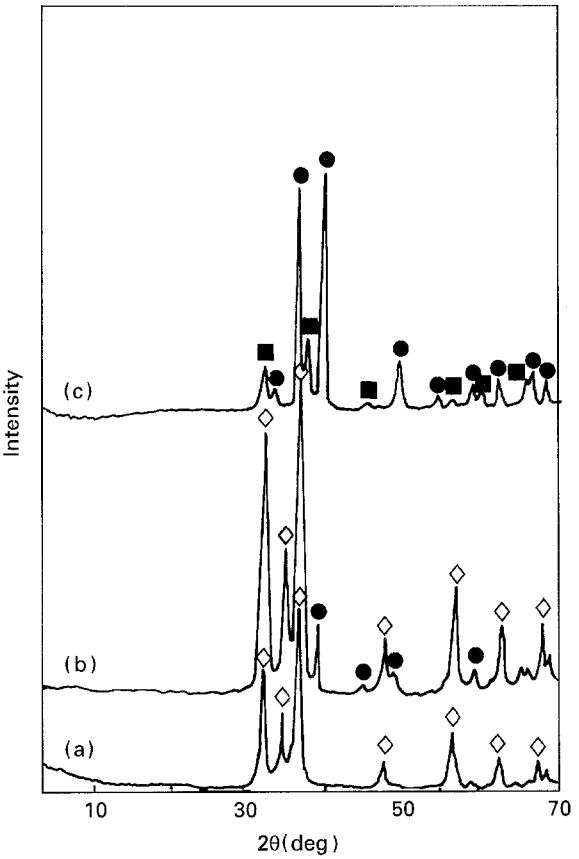

Figure 5 Powder X-ray diffraction patterns of (a) sample A3, (b) sample C12, and (c) sample C14 obtained upon calcination at 973 K: (◇) ZnO, (●) CuO, (■) MAl_2O_4, M = Zn, Cu.

but the metal oxide is still the major compound in the calcined products.

In the range 573–773 K, even small quantities of zinc, clearly decreases the thermal stability of the hydrotalcite compounds, as the metal oxide phases appear at lower temperatures compared to the Mg–Al system.

The thermal behaviour of the Zn–Cu–Al system is different to the Mg–Zn–Al system described above. The disappearance of the hydrotalcite PXRD pattern can be observed at temperatures lower than 473 K. Total destruction of the hydrotalcite structure and formation of phases similar to metal oxides is detected. ZnO forms with a low copper content, both ZnO and CuO are detected at Cu/Zn ratios smaller than two, and the only CuO phase is observed at high Cu/Zn ratios. The peaks of the metal oxide-like phase become sharp at 773 K. As noted in the Mg–Zn–Al system, the metal oxide phases contain on aluminium cation, substituted in the unit structure and verified by the shift of the cell parameters to lower values, compared to that of pure oxides. At 973 K, in addition to the metal oxide phases, a spinel form is detected at a Cu/Zn ratio higher than two. Fig. 5 indicates that the presence of the copper ion in the solid solution decreases the decomposition temperature of the hydrotalcite compounds, and accelerates the formation of the spinel phase at temperatures less than 973 K, and is accompanied by an exothermic peak around 953 K. In the Zn–Al system only zinc oxide is detected at temperatures lower than 1123 K.

Between 1023–1273 K, the intensities of the characteristic peaks of the spinel phase (MAl_2O_4, M = Zn, Cu) increase, due to interaction between aluminium and oxide-like phases, but the metal oxide phases remain dominantly in the calcined materials.

4. Conclusions

This investigation illustrates that hydrotalcite-like compounds are obtained in both Mg–Zn–Al and Zn–Cu–Al systems with carbonate anions. But the copresence of another phase depends on the starting compositions of the ion solutions. The reactivity of the zinc cation depends also on the other coexistent cation; this cation precipitates easily in the Zn–Cu–Al system, however, precipitation is not complete in the Mg–Zn–Al system.

The Zn–Cu–Al hydrotalcite-like compounds have a lower thermal stability at 473 K, reflected by the disappearance of the hydrotalcite PXRD pattern, compared to the Mg–Zn–Al compounds, which are stable at temperatures higher than 473 K. Interaction between the aluminium ion and metal oxide phases occurs at temperatures around 973 K in the case of the Zn–Cu–Al system; however, the spinel phase is only detected in the Mg–Zn–Al system at temperatures higher than 1123 K.

Acknowledgements

The authors wish to thank Dr J.L. Dubois from the National Chemistry Laboratory for Industry, Tsukuba for helpful discussions and Dr W. Jones from the Department of Chemistry, Cambridge for suggestions

made concerning this paper. F.K. thanks JISTEC for financial support as an STA fellowship.

References

1. M. C. GASTUCHE, G. BROWN and M. M. MORTLAND, *Clay Miner.* **7** (1967) 177.
2. R. ALLMANN, *Chimica* **24** (1970) 99.
3. S. MIYATA, *Clays & Clay Miner.* **23** (1975) 369.
4. F. THEVENOT, R. SZYMANSKI and P. CHAUMETTE, *ibid.* **37** (1989) 396.
5. C. J. SERNA, J. L. RENDON and J. E. IGLESIAS. *ibid.* **30** (1982) 180.
6. R. ALLMANN, *Acta Crystallogr.* **B24** (1968) 972.
7. H. F. W. TAYLOR, *Miner. Mag.* **37** (1969) 338.
8. W. T. REICHLE, *Chem. Technol.* January **16** (1986) 58.
9. F. CAVANI, F. TRIFIRO and A. VACCARI, *Catal. Today* **11** (1991) 173.
10. F. KOOLI, K. KOSUGE, T. HIBINO and A. TSUNASHIMA, *J. Mater. Sci.* **28** (1993) 2769.
11. G. W. BRINDLEY and S. KIKKAWA. *Am. Mineral.* **64** (1979) 836.
12. E. B. M. DOESBURG, R. H. HOPPENER, B. DE KONING, XU. XIAO DING and J. J. F. SCHOLTEN, "Preparation of Catalysis IV", edited by B. Delmon, P. Grange, P. A. Jacobs and G. Pancelet (Elsevier, Amsterdam, 1987) pp. 767.
13. K. HASHI, S. KIKKAWA and M. KOIZUMI, *Clays & Clay Miner.* **31** (1983) 152.
14. C. BUSETTO, G. DEL PIERO, G. MANARA, F. TRIFIRO and A. VACCARI, *J. Catal.* **85** (1984) 260.
15. L. PAUSCH, H. LOHSE, K. SCHURMANN and R. ALLMANN, *Clays & Clay Miner.* **34** (1986) 507.
16. G. BROWN and M. C. CASTUCHE, *Miner. Mag.* **36** (1967) 193.
17. G. MASCOLO and O. MARINO, *ibid.* **43** (1980) 619.
18. R. D. SHANNON, *Acta Crystallogr.* **A32** (1976) 751.
19. F. M. LABAJOS, V. RIVES and M. A. ULIBARRI, *Spectrosc. Lett.* **24** (1991) 499.
20. P. C. ROUXHET and H. F. W. TAYLOR, *Chimica* **23** (1959) 480.
21. T. SATO, H. FUJITA, T. ENDO, M. SHIMADA and A. TSUNASHIMA, *Reactivity Solids* **5** (1988) 219.
22. C. W. BECK, *Am. Mineral.* **35** (1950) 1006.
23. M. J. HERNANDEZ-MORENO, M. A. ULIBARRI, J. L. RENDON and C. J. SERNA, *Phys. Chem. Miner.* **12** (1985) 34.
24. D. L. BISH and G. W. BRINDLEY, *Am. Mineral.* **62** (1977) 458.
25. D. L. BISH, *Bull. Mineral.* **103** (1980) 170.
26. P. TARTE, *Spectrochim. Acta* **23A** (1967) 2127.

Received 11 July 1994
and accepted 11 April 1995